A hybrid modal/statistical formulation for predicting the energy response of vibroacoustic systems in the mid frequency range

Guang Zhu, Laurent Maxit, Nicolas Totaro, Alain Le Bot

A hybrid modal/statistical formulation for predicting the energy response of vibroacoustic systems in the mid frequency range

Guang Zhu[a,b,*], Laurent Maxit[a], Nicolas Totaro[a], Alain Le Bot[b]

[a] *Univ Lyon, INSA Lyon, LVA, EA677, 69621 Villeurbanne, France*
[b] *Univ Lyon, Ecole Centrale de Lyon, LTDS, CNRS UMR 5513, 69134 Ecully, France*

Abstract

The Statistical modal Energy distribution Analysis (SmEdA) method predicts the power flow between coupled subsystems excited by random excitations from a deterministic modal description of the uncoupled subsystems. As the modes can be computed by Finite Element Method (FEM) for complex subsystems, it can be seen as an extension of FEM to the mid frequency range where the modal densities of subsystems are not too high. Conversely, the Statistical Energy Analysis (SEA) method is a statistical approach predicting the mean power flow of a population of similar structures presenting manufacturing uncertainties. Assuming a diffuse field within each subsystem, it is dedicated to the high frequency range where modal densities of subsystems are high. However, in many applications, subsystems with low and high modal densities can coexist in the mid frequency range and in that case neither SmEdA nor SEA is well adapted. The purpose of this article is then to propose a hybrid SmEdA/SEA formulation allowing some subsystems with low modal densities to be described by SmEdA and other ones by SEA. For the SEA-described subsystems, the vibratory field of the statistical population is supposed to be diffuse. These subsystems are then characterized by sets of natural frequencies and mode shapes constructed from the Gaussian Orthogonal Ensemble matrix and the cross-spectrum density of a diffuse field, respectively. In another hand, the SmEdA-described subsystems are represented by their modes that can be extracted by usual computer codes. In order to couple the two models, Monte Carlo simulations are used for generating samples of the stochastic modes of the SEA-described subsystems. From the distribution of the estimated energy response of the coupled subsystems, the ensemble average and the confidence interval can finally be estimated. For validation purpose, the results of the proposed hybrid SmEdA/SEA approach are compared to the numerical results computed with the finite element method (FEM) on a population of plate-cavity systems having similar properties. A good agreement is observed whereas the computation time of the proposed approach is much less important than the one of the FEM which can be up to several days for each element of the population.

Keywords: statistical vibro-acoustic modeling; hybrid SmEdA/SEA; ensemble-averaged response; diffuse field.

1. Introduction

The vibroacoustic response of complex engineering systems under broadband sources of noise and vibration is of interest in many applications. Several methods have been developed including deterministic and statistical approaches. In the low frequency domain, methods such as Finite Element Method (FEM) [1] and Boundary Element Method (BEM) [2] are well adapted for deterministic systems under pure tone excitation. In the high frequency domain, uncertainties and randomnesses introduced by manufacturing and material imperfections that widely exist in engineering structures can highly affect the vibration field [3], which makes the deterministic modeling difficult and in some cases meaningless. Consequently, describing the vibrational behavior of each subsystem statistically with averaged energy variables becomes more appropriate (e.g. the averaged interior noise for a fleet of cars manufactured on the same production line). The most widely used energy-based approach is the Statistical Energy Analysis (SEA).

SEA was developed for predicting the vibration and noise transmission in complex systems at high frequency [4, 5, 6]. In classical SEA, a complex system is divided into subsystems and the power flow exchanged between two coupled subsystems is related to the vibration energy of each subsystem via the Coupling Loss Factor (CLF). The response is described in terms of the "mean" energy level in each subsystem. Strictly speaking, the system is considered to have random properties and the output "mean" energy is interpreted as the average taken over a population of systems which share similar characteristics but differ in details to have randomly distributed parameters [7]. Sometimes, the "mean" energy can also be interpreted as a frequency-averaged value taken on one particular deterministic realization of the system. In this case, the output can be affected by its specific mode shapes and natural frequency distribution [8]. If the vibration field is diffuse (constant energy density) and the studied frequency band is wide enough to encompass a sufficient number of resonant modes in each subsystem, a frequency average taken on any particular deterministic realization of the system yields the same result as an ensemble average. The application of energy power flow balance for one individual deterministic system is often termed as SEA-like [9] and this terminology will be used in the present article.

To deal with the mid frequency range where neither SEA nor deterministic approaches are applicable, alternative methods are developed over the past years, for example, the Statistical modal Energy distribution Analysis (SmEdA)[10, 11, 12]. SmEdA is developed as an extension of the classical SEA [13, 14]. It extends the validity domain of SEA to lower frequency by removing the modal energy equipartition assumption [15, 16]. In SmEdA, the vibration field of each coupled subsystem is characterized by uncoupled modes and the power exchanged between two modes of the coupled subsystem is proportional to the difference of their modal energies. Writing the power balance equation for all the modes in each subsystem produces a system

*Corresponding author
Email address: guang.zhu@insa-lyon.fr (Guang Zhu)

of linear equations where the unknowns are the modal energies of subsystems. SmEdA is well adapted to the mid frequency range where the studied subsystems are having low modal density so diffuse vibration field is difficult to achieve. In addition, it requires much less computation time and resources than finite element method. However, it only delivers a frequency averaged response of one particular realization, which is not necessarily the same as an ensemble average. For a complex vibro-acoustic system that contains both low modal density and high modal density subsystems (e.g. a structure/cavity system), the frequency averaged responses show a large variability (demonstrated in sec 4.3) as the frequency average of one specific realization is affected by the mode shapes and natural frequency distribution, which is sensitive to the uncertainty and randomness in the subsystems. In that case, the prediction of ensemble averaged response seems more meaningful.

To study the vibro-acoustic system having different dynamic behavior in different subsystems, hybrid approaches which use deterministic method to study the low modal density subsystem and SEA to study the high modal density subsystem are developed. The hybrid finite element-statistical analysis is one of the most representative ones which allows modeling small components (compared to a wavelength) using FEM and large ones statistically by SEA (FE-SEA) [17, 18]. In FE-SEA, the coupling between the deterministic and statistical subsystems is established by using the "diffuse field reciprocity relation", and the ensemble averaged response of the system is solved at each frequency [19]. Benefit from the FE, the hybrid FE-SEA approach has strong applicability especially when the deterministic subsystems have complex shapes. However, it should also be noted that FE-SEA can be time-consuming as it requires computing the inverse of the total dynamic stiffness matrix at each frequency [20].

In this context, the present work proposes a hybrid SmEdA/SEA method for predicting the energy response of a complex vibro-acoustic system that contains both low modal density subsystems and high modal density subsystems. It allows computing the energy response of the system by describing low modal density subsystems by their deterministic modes (as in SmEdA) and the high modal density subsystems with a stochastic diffuse field (as in SEA). A stochastic diffuse field can be considered as a random field, with which the effect of uncertainty and randomness induced by local scattering is considered without explicitly indicating their source and detailed parameters. As frequency goes up, the probability distribution of the normalized eigenvalue spacing for any diffuse vibro-acoustic subsystem conforms to that of the Gaussian Orthogonal Ensemble (GOE), and its acoustic mode shapes are a zero-mean Gaussian random field [21, 22]. Then the modal frequencies of the subsystem exhibiting a diffused field can be estimated from the GOE matrix whereas the mode shapes can be constructed in order to comply with the cross-spectrum density of a diffuse field. Realizations of these modes shapes can be obtained by a spatial approach based on a Cholesky decomposition [21] or a wavenumber approach based on the UWPW (Uncorrelated wall plane waves) decomposition [23]. A Monte Carlo simulation can be established with a set of hybrid SmEdA/SEA-Like models. Each sample consists of one realization of the stochastic subsystem that is represented by a

SEA-Like model whereas the deterministic subsystem is represented by SmEdA with its deterministic modes. The proposed hybrid SmEdA/SEA formulation permits not only the computation of the ensemble-averaged energy response but also the confidence interval generated by the uncertainties and randomness without bringing in much computation.

The outline of this paper is as follows. For sake of conciseness and simplification, it is assumed in the following that the low modal density deterministic subsystem is a thin structure whereas the high modal density stochastic subsystem is an uncertain acoustic cavity although the proposed approach can be generalized to any type of system containing deterministic and stochastic subsystems. In section 2, the governing equations for a SmEdA model of a structure/cavity system are reminded before deriving the SmEdA/SEA-Like model by relaxing the modal energy equipartition assumption. The relations between SmEdA, SEA-Like, and hybrid SmEA-SEA are discussed. Section 3 describes the statistical model characterizing the stochastic subsystem, namely the Gaussian Orthogonal Ensemble (GOE) and the Cross Spectral Density (CSD) of a diffuse field. The process for generating realizations of the modal frequencies and the mode shapes are then described as well as the Monte Carlo process leading to the hybrid SmEdA/SEA model. In section 4, the accuracy of the proposed approach is studied by comparing its results with the ones obtained by finite element simulations on an ensemble of plate-cavity systems.

2. Governing equations of SmEdA and SEA-Like methods

2.1. SmEdA description of subsystems

SmEdA was derived by Maxit and Guyader [24] from a Dual Modal Formulation (DMF). This latter permits to represent the coupling between two subsystems from the uncoupled subsystem modes. Details on the fundaments of DMF can be found in the section 3 of [15] as well as in the appendix A of [25]. One of the subsystems has to be described in term of displacements with its uncoupled-free modes whereas the other one has to be described in term of stress with its uncoupled-blocked modes on the coupling area. Moreover, when a mechanical impedance mismatch occurs at the coupling interface between the two subsystems, the stiffer subsystem should be described by the uncoupled-free modes whereas the softer one should be described by the uncoupled-blocked modes to ensure that the resonant subsystem modes are able to represent the behaviour of the coupled subsystem in the considered frequency band of excitation (see the numerical results of DMF in [16]).

Let us consider a plate - air cavity system. The plate being the stiffer part of the system, it should be described in the DMF by its normal displacements and its (in-vacuo) modes (which correspond to the uncoupled-free modes, the modes of the plate with null stresses applied on the coupling boundary with the cavity) whereas the cavity is described in term of pressure (i.e. normal stress) and its modes with rigid walls (which correspond to the uncoupled-blocked modes, the modes of the cavity with null displacements

applied on the coupling boundary with the plate). Details on the DMF on this case can be found in [26]. The coupling between the plate and the cavity can then be described by the interaction between two set of modes as illustrated in Fig. 1

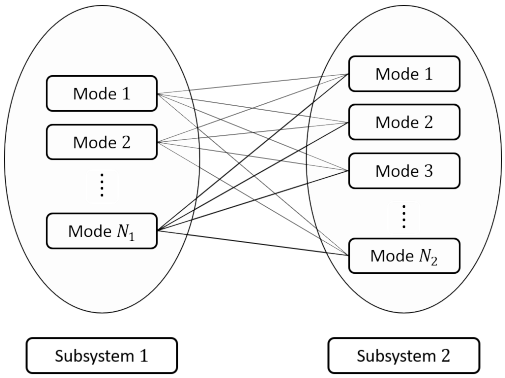

Figure 1: Illustration of the modal interactions between the plate (subsystem 1) and the cavity (subsystem 2)

Assuming the coupling between subsystems is weak and that the external excitations are uncorrelated white noises, the frequency average power flow Π_{pq} between mode p of subsystem 1 and mode q of subsystem 2 is proportional to the difference in their frequency average modal energies as

$$\Pi_{pq} = \beta_{pq} \left(E_p - E_q \right), \tag{1}$$

where E_p and E_q are the modal energies of mode p of subsystem 1 and mode q of subsystem 2. The coupling coefficient between mode p and mode q, β_{pq}, can be expressed in terms of the modal information as [27]

$$\beta_{pq} = \frac{(W_{pq})^2}{M_p M_q} \left[\frac{\eta_p \omega_p \omega_q^2 + \eta_q \omega_q \omega_p^2}{\left(\omega_p^2 - \omega_q^2\right)^2 + (\eta_p \omega_p + \eta_q \omega_q)(\eta_p \omega_p \omega_q^2 + \eta_q \omega_q \omega_p^2)} \right], \tag{2}$$

where M_p, ω_p, η_p and M_q, ω_q, η_q are respectively the modal mass, natural frequency, and modal damping loss factor of mode p of subsystem 1 and mode q of subsystem 2. W_{pq} is the interaction modal works between the p^{th} displacement mode shape w_p of the plate (with free boundary condition of the coupling area Σ) and the q^{th} pressure mode shape σ_q of the cavity (with rigid walls),

$$W_{pq} = \int_{\Sigma} w_p \, \sigma_q dS. \tag{3}$$

For each mode of each subsystem, the principle of energy conservation yields the power balance as

$$\begin{aligned} \Pi_{\text{inj}}^p &= \Pi_{\text{diss}}^p + \sum_{q=1}^{N_2} \Pi_{pq}, \quad \forall p \in [1, N_1], \\ \Pi_{\text{inj}}^q &= \Pi_{\text{diss}}^q - \sum_{p=1}^{N_1} \Pi_{pq}, \quad \forall q \in [1, N_2], \end{aligned} \tag{4}$$

in which Π^p_{inj} (resp.Π^q_{inj}) represents the frequency average power injected in the p^{th} (resp. q^{th}) mode of subsystem 1 (resp. subsystem 2). For a white noise point force applied on the plate at point M_e, the injected powers in the cavity modes are null (i.e. $Pi^q_{\text{inj}} = 0$) whereas the injected powers in the plate modes are obtained by

$$\Pi^p_{inj} = \frac{\pi}{4M_p} w_p^2(M_e) S_{FF}, \tag{5}$$

where S_{FF} is the power spectral density of the generalized force expressed in N^2/rad/s and $w_p(M_e)$ is the p^{th} displacement mode shape at the excitation point M_e. $\Pi^p_{\text{diss}} = \eta_p \omega_p E_p$ and $\Pi^q_{\text{diss}} = \eta_q \omega_q E_q$ are the powers dissipated by the p^{th} mode of subsystem 1 and q^{th} mode of subsystem 2. $\sum_{q=1}^{N_2} \Pi_{pq}$ is the power flow exchanged between the p^{th} mode of subsystem 1 and all the modes of subsystem 2, and $\sum_{p=1}^{N_1} \Pi_{pq}$ is the power flow exchanged between the q^{th} mode of subsystem 2 and all the modes of subsystem 1.

Substitution of Eq. (1) into Eq. (4) gives a system of linear equations

$$\begin{aligned}
\Pi^p_{\text{inj}} &= \left(\eta_p \omega_p + \sum_{q=1}^{N_2} \beta_{pq} \right) E_p - \sum_{q=1}^{N_2} \beta_{pq} E_q, \quad \forall p \in [1, N_1], \\
\Pi^q_{\text{inj}} &= -\sum_{p=1}^{N_1} \beta_{pq} E_p + \left(\sum_{p=1}^{N_1} \eta_q \omega_q + \beta_{pq} \right) E_q, \quad \forall q \in [1, N_2].
\end{aligned} \tag{6}$$

Finally, solving this system of equations gives modal energies E_p and E_q of both subsystems. The total energy of each subsystem can be obtained by summing all the modal energies in the studied frequency band as

$$E_1 = \sum_{p=1}^{N_1} E_p, \quad E_2 = \sum_{q=1}^{N_2} E_q, \tag{7}$$

where E_1 and E_2 are the total energies of subsystems 1 and 2 averaged in the frequency band of interest. One should also notice that the system of equations (6) contains $N_1 + N_2$ modes. Consequently, in the high frequency range and for some kind of subsystems (for example acoustic cavities), the system of equations to solve can become time consuming as the number of modes quickly increases. For this kind of subsystems, a SEA-like approach can become more adapted.

2.2. SEA-like description of subsystems

A SEA-like description of deterministic subsystems can be derived from SmEdA under the assumption of modal energy equipartition. With this hypothesis, all the modes of a subsystem have an equal value defined as,

$$E_p = \frac{E_1}{N_1}, \quad E_q = \frac{E_2}{N_2}. \tag{8}$$

Introducing this relation into Eq. (6) and summing the modal energy conservation equation for each subsystem yields the energy balance equations of a SEA-like method

$$\begin{aligned} \Pi^1_{\text{inj}} &= \omega_c \eta_1 E_1 + \omega_c \left(\eta_{12} E_1 - \eta_{21} E_2\right), \\ \Pi^2_{\text{inj}} &= \omega_c \eta_2 E_2 + \omega_c \left(\eta_{21} E_2 - \eta_{12} E_1\right), \end{aligned} \tag{9}$$

where $\Pi^1_{\text{inj}} = \sum_{p=1}^{N_1} \Pi^p_{\text{inj}}$, $\Pi^2_{\text{inj}} = \sum_{q=1}^{N_2} \Pi^q_{\text{inj}}$ represent the total power injected into subsystem 1 and subsystem 2 respectively. The coupling loss factors η_{12} and η_{21} characterising the power flow between two subsystems are calculated with

$$\eta_{12} = \frac{1}{N_1 \omega_c} \sum_{p=1}^{N_1} \sum_{q=1}^{N_2} \beta_{pq}, \qquad \eta_{21} = \frac{1}{N_2 \omega_c} \sum_{p=1}^{N_1} \sum_{q=1}^{N_2} \beta_{pq}. \tag{10}$$

When SEA-like is employed for one single system, the underlying assumption implies that energy equipartition is fulfilled for all the subsystems. In real applications, this can be difficult to fulfill as some subsystems can exhibit a modal behavior not compatible with the modal energy equipartition assumption.

3. Derivation of a hybrid SmEdA/SEA formulation

3.1. Hybrid SmEdA/SEA-Like method

For applications where subsystems with low and high modal densities coexist, it is possible to mix a SmEdA description for some subsystems and a SEA description for the others. This is done in a quite straightforward way by assuming modal energy equipartition as done in section 2.2 but only for some subsystems. For example, consider that subsystem 1 can be described by its deterministic modes (because of a low modal density for example) while subsystem 2 can only be described by global quantities (because of a too high modal density for example). In that case, the modal energy equipartition is only assumed for subsystem 2

$$\begin{aligned} \Pi^p_{\text{inj}} &= \left(\eta_p \omega_p + N_2 \gamma_p\right) E_p - \gamma_p E_2, \qquad \forall p \in [1, N_1], \\ \Pi^2_{\text{inj}} &= -\sum_{p=1}^{N_1} N_2 \gamma_p E_p + \left(\sum_{p=1}^{N_1} \gamma_p + \eta_2 \omega_c\right) E_2, \end{aligned} \tag{11}$$

where

$$\gamma_p = \frac{1}{N_2} \sum_{q=1}^{N_2} \beta_{pq} \tag{12}$$

represents the averaged modal coupling coefficient between mode p of subsystem 1 and all the modes of subsystem 2 in the frequency band of interest.

In this hybrid formulation, the unknowns are either the modal energies (here for subsystem 1) or the global energy (here for subsystem 2) of the coupled subsystems. However, the modal or global energy responses from the above formulation are frequency averages taken from a single deterministic system. In addition,

computing Eq. (12) still relies on modal coupling loss factor calculation and so on the modal information of the cavity. Even if this formulation shows that mixing a SmEdA description for some subsystems to a SEA description for the others, it is only a post-process of SmEdA formulation. The difficulty arises here from the estimation of the average coupling loss factor γ_p which depends on natural frequencies and mode shapes of both subsystems (see Eq. (2)). In the next section, the concept of an *equivalent stochastic subsystem* is introduced. In that approach, the deterministic natural frequencies and mode shapes of the SEA-described subsystems are replaced by a theoretical diffuse field based on statistical information.

3.2. Equivalent stochastic subsystems

The SEA description of a subsystem implies the appearance of a diffuse field in the subsystem but also that the global energy of the subsystem is the energy expectation over a population of nearly identical subsystems and not the energy of a particular element of the population. Let us consider the example in Fig. 2, a thin structure is excited by a random force F of white-noise type at the position M_e and coupled with a cavity with uncertain boundaries and containing a rigid body located at a random position. Let consider that a diffuse field and so the modal energy equipartition could never be reached for the structure subsystem. In that case, a deterministic SmEdA description is well adapted. Conversely, even though the cavity is only subject to surface excitation from the vibrating structure, homogeneity, and isotropy of the acoustic field can be guaranteed from one hand by the shape of the cavity which can exhibit ergodicity property [28] and for another hand by the random position of the rigid object and the small variations of the cavity shapes from one system to another one. In this situation, the acoustic field in the cavity can be reasonably supposed to be diffuse over the statistical population. It results that the subsystem can be characterized by these properties of diffuseness of its acoustic field instead of describing it by the uncertain geometrical and physical parameters. In the following, an *equivalent stochastic subsystem* will be defined as a subsystem in which a diffuse field is assumed (as for the cavity in the present example). Therefore, for each sample of this *equivalent stochastic subsystem*, the modal frequencies and the mode shapes on the coupling surface used in Eq. (12) should be estimated in order to construct a SmEdA/SEA-like model corresponding to this sample. If the geometry of the stochastic subsystem does not exhibit symmetries, the probability distribution of the local eigenvalue spacings tends to the one of the Gaussian Orthogonal Ensemble (GOE) matrix, and its mode shapes can be considered as a zero-mean Gaussian random field and comply with the cross-spectrum density function of a diffuse field. The process for generating the modal frequencies is described in section 3.2.1 whereas those for the mode shapes are presented in the section 3.2.2. Finally, a Monte Carlo process is applied to deduce the mean and the confidence interval of the energy responses from the estimations with the SmEdA/SEA-like models. This process leads to the so-called hybrid SmEdA/SEA model as resumed in section 3.3.

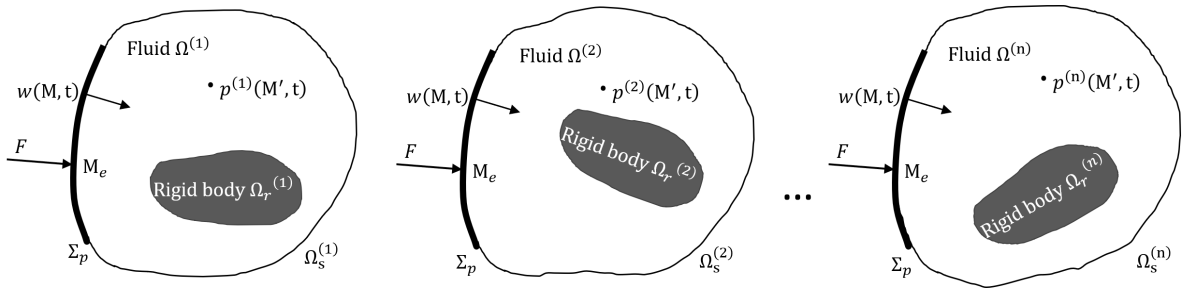

Figure 2: Illustration of three samples of the uncertain vibroacoustic system characterized by a cavity with uncertain boundary conditions and an internal rigid body at an arbitrary position.

3.2.1. Natural frequencies of the equivalent stochastic cavity

Let us considered the equivalent stochastic cavity of volume V and of the sound speed c. The modal density of the cavity for the frequency band $[\omega_l, \omega_u]$ of central frequency ω_c can be estimated from the analytical expression, [5]:

$$n(\omega_c) = \frac{\omega_c^2 V}{2\pi^2 c^3}. \tag{13}$$

The expected number of modes in the considered frequency band can then be deduced and expressed as:

$$N_e = n(\omega_c)\,(\omega_u - \omega_l). \tag{14}$$

To construct the natural frequencies of the stochastic cavity, it is supposed that the probability distribution of the local eigenvalue spacing of the equivalent stochastic cavity tends to the one of a GOE matrix [21, 22]. This type of matrix is real and symmetric with random entries that can be written as [1]

$$\mathbf{G}_{n_\mathrm{G}}(\sigma_\mathrm{G}) := \begin{bmatrix} \mathrm{G}_{11} & \mathrm{G}_{12} & \dots & \mathrm{G}_{1n_\mathrm{G}} \\ \mathrm{G}_{12} & \mathrm{G}_{22} & \dots & \mathrm{G}_{2n_\mathrm{G}} \\ \vdots & \vdots & \ddots & \vdots \\ \mathrm{G}_{1n_\mathrm{G}} & \mathrm{G}_{2n_\mathrm{G}} & \dots & \mathrm{G}_{n_\mathrm{G}n_\mathrm{G}} \end{bmatrix}, \tag{15}$$

where n_G represents the number of rows and columns. Entries in the GOE matrix are independent Gaussian random variables, the ones on the diagonal having a variance $2\sigma_\mathrm{G}^2$ and the off-diagonal ones having a variance σ_G^2. As matrix $\mathbf{G}_{n_\mathrm{G}}(\sigma_\mathrm{G})$ is real and symmetric, it has n_G eigenvalues $\lambda_{\mathrm{G}r}$, which are real and centered around zero, and the density of the GOE eigenvalues, for $n_\mathrm{G} \gg N_e$, converges to

$$n_\mathrm{G}^\lambda(\lambda_\mathrm{G}) = \frac{2n_\mathrm{G}}{\pi r}\sqrt{1 - \frac{\lambda_\mathrm{G}^2}{r^2}}, \quad -r < \lambda_\mathrm{G} < r, \tag{16}$$

with $r := 2\sigma_\mathrm{G}\sqrt{n_\mathrm{G}}$. In the following numerical calculation, n_G is set to be ten times N_e. The normalized eigenvalue spacings s_Gr of the GOE are defined as,

$$s_\mathrm{Gr} := n_\mathrm{G}^\lambda(\lambda_{\mathrm{G}0})\,(\lambda_{\mathrm{G}r} - \lambda_{\mathrm{G}0}), \tag{17}$$

[1] := means that the item on the left-hand side is being defined to be what is on the right-hand side.

where $\lambda_{\mathrm{G}0}$ is an arbitrary but fixed value for all the GOE eigenvalues $\lambda_{\mathrm{G}r}$ ($\lambda_{\mathrm{G}0} = 0$ is chosen in the following).

In another hand, for the equivalent stochastic cavity, the r^{th} normalized eigenvalue spacing is given by

$$s_r := n^{\lambda}(\lambda_c)\,(\lambda_r - \lambda_l)\,, \tag{18}$$

where $\lambda_l = \omega_l^2$. $n^{\lambda}(\lambda_c)$ represents the eigenvalue density of the equivalent stochastic cavity at the central angular frequency ω_c ($\lambda_c = \omega_c^2$) and it is related by the modal density $n(\omega_c)$ [21]

$$n^{\lambda}(\lambda_c) = n^{\lambda}\left(\omega_c^2\right) = \frac{n(\omega_c)}{2\omega_c}. \tag{19}$$

The r^{th} acoustic eigenvalue λ_r of the equivalent stochastic cavity in the frequency band of interest can be expressed as,

$$\lambda_r = \frac{s_r}{n^{\lambda}(\lambda_c)} + \lambda_l \text{ as long as } \lambda_r < \lambda_u. \tag{20}$$

The realization of λ_r can be related to the GOE matrix by imposing the normalized eigenvalue spacings s_r to be the same as those of the GOE matrix $s_{\mathrm{G}r}$. The r^{th} modal frequency ω_r of the equivalent stochastic cavity can finally be obtained by:

$$\omega_r = \sqrt{2\omega_c \frac{s_{\mathrm{G}r}}{n(\omega_c)} + {\omega_l}^2} \text{ as long as } \omega_r < \omega_u. \tag{21}$$

In conclusion, the synthesis of the modal frequencies of the cavity in the frequency band of interest can be decomposed in 4 steps:

- First, evaluation of the number of expected modes using Eq. (14);
- Second, construction of a GOE matrix of dimension ten times the number of expected modes;
- Third, extraction of the eigenvalues of the GOE matrix and estimation of the eigenvalue spacings with Eq. (17);
- Last, calculation of the modal frequencies with Eq. (21);

3.2.2. Mode shapes of an equivalent stochastic cavity

Here, it is supposed that the mode shapes of the equivalent stochastic cavity can be considered as a zero-mean Gaussian random field and that they comply to the cross-spectrum density function of a diffuse field. The methods of mode shapes realization of the diffuse field has been studied by many researchers, a brief review is presented here to introduce the mode shape realization with spatial approach [21, 22] and wavenumber approach [29, 30]. The obtained mode shapes are required for the calculation of modal interaction works W_{pq} (see Eq. (3)). The integral in the definition of W_{pq} will be estimated with the rectangular rule. Hence, the coupling surface is discretized by a regular grid of Θ points $\mathbf{x}_i, i \in [1, \Theta]$. A

mode shape vector containing the r^{th} realization of the modal pressure on the coupling surface is defined as,

$$\boldsymbol{\varphi}_r := \left[\varphi_r\left(\mathbf{x}_1\right)\ \varphi_r\left(\mathbf{x}_2\right)\ \ldots\ \varphi_r\left(\mathbf{x}_\Theta\right)\right]^T, \tag{22}$$

considering statistical properties of an acoustic diffuse field. The Cross Spectrum Density (CSD) of the modal pressure at two different positions is then given by

$$\mathrm{G}_{\varphi_r\varphi_r}\left(\mathbf{x}_i, \mathbf{x}_j\right) = \mathrm{E}\left[\varphi_r(\mathbf{x}_i)\varphi_r(\mathbf{x}_j)\right] = S_{\varphi_r\varphi_r}\overline{G}_{DAF}\left(\mathbf{x}_i - \mathbf{x}_j\right), \tag{23}$$

where

- $S_{\varphi_r\varphi_r}$ is the Auto Spectrum Density (ASD) of the blocked pressure on the coupling surface which is independent of the point $\mathbf{x}_i, i \in [1, \Theta]$ as the process is spatially homogeneous,
- $\overline{G}_{DAF}\left(\mathbf{x}_i - \mathbf{x}_j\right)$ is the normalized CSD of a diffuse acoustic field defined by [31, 32]

$$\overline{G}_{DAF}(\Delta\mathbf{x}) = \frac{\sin\left(k_0\|\Delta\mathbf{x}\|\right)}{k_0\|\Delta\mathbf{x}\|}, \tag{24}$$

where $k_0 = \frac{\omega_c}{c_0}$ is the acoustic wavenumber at the central frequency of the considered frequency band.

The mass (or strain energy) of the random cavity mode for the r^{th} realization is defined by

$$M_r = \frac{1}{\rho_0 c_0^2}\int_\Omega \varphi_r^2(\mathbf{x})d\mathbf{x}. \tag{25}$$

Normalizing the mode shapes such that the expectation of the modal mass (i.e. ensemble averaged on the different realizations) is equal to one (i.e. $E\left[M_r\right]_k = 1$) leads to the expression of the space average of the expectation of the quadratic modal pressure

$$\left\langle\varphi_r^2\right\rangle_\Omega = \frac{1}{V_\Omega}\int_\Omega E\left[\varphi_r^2(\mathbf{x})\right]_k d\mathbf{x} = \frac{\rho_0 c_0^2}{V_\Omega}. \tag{26}$$

According to Sabine's assumptions [33], for a standard diffuse field, a ratio of 2 occurs between the ASD of the blocked pressure and the space average of the quadratic pressure. It results that

$$S_{\varphi_r\varphi_r} = \frac{2\rho_0 c_0^2}{V_\Omega}. \tag{27}$$

Eq. (23) and Eq. (27) define the CSD of the modal pressure such that the acoustic field is diffuse and the mode shapes are normalized to one. In the following, two numerical processes to synthetize realizations of these modal pressures complying with these two equations are presented:

- Spatial approach:

  Consider an eigendecomposition of the cross spectral matrix of the modal pressure

$$\mathbf{G}_{\varphi_r\varphi_r} = \left[G_{\varphi_r\varphi_r}\left(\mathbf{x_i}, \mathbf{x_j}\right)\right]_{\Theta\times\Theta} = \mathbf{P}\boldsymbol{\Gamma}\mathbf{P}^{\mathrm{T}}, \tag{28}$$

where $\mathbf{\Gamma}$ is a diagonal matrix containing the eigenvalues and $\mathbf{P}$ is a full matrix containing the eigenvectors. The blocked pressure vector of the r^{th} realization is then obtained by [21, 22]

$$\boldsymbol{\varphi}_r = \mathbf{P}\mathbf{\Gamma}^{\frac{1}{2}}\zeta_r, \tag{29}$$

where $\Gamma^{\frac{1}{2}}$ is a diagonal matrix containing the square root of the eigenvalues of Γ, and ζ_r is a vector of Θ standard normal random variables that can be realized with a Gaussian random number generator.

- Wavenumber approach:

The spatial Fourier transform of the normalized CSD of a diffuse field $\overline{G}_{DAF}$ is [29]

$$\tilde{G}_{DAF}(\mathbf{k}) = \begin{cases} \frac{2\pi}{k_0}\frac{1}{\sqrt{k_0^2 - \|\mathbf{k}\|^2}}, & \text{if } \|\mathbf{k}\| < k_0, \\ 0, & \text{otherwise .} \end{cases} \tag{30}$$

Only components inside the acoustic wavenumber domain (i.e.$\|\mathbf{k}\| < k_0$) are not null. Let discretise this domain with a wavenumber, δ_k in both wavenumber directions. Φ_k represents the discretized acoustic wavenumber domain. Taking into account the ASD of the blocked pressure given by Eq.(27), the blocked pressure vector of the rth realization is then obtained by [23, 30]

$$\varphi_r(\mathbf{x}) = \frac{\sqrt{\rho_0}c_0\delta_k}{\sqrt{2V_\Omega\pi}} \sum_{\zeta\in\Phi_k} \sqrt{\overline{G}_{DAF}\left(\mathbf{k}_\zeta\right)} e^{i\zeta_r^\varsigma} e^{i\mathbf{k}_\zeta\mathbf{x}}, \quad \mathbf{x}\in\Sigma_p, \tag{31}$$

where ζ_r^ς is the phase attributed to the ς^{th} wall plane wave for the r^{th} realization and corresponds to a random value uniformly distributed in $[0, 2\pi]$. The wavenumber approach avoids the eigendecomposition of the spatial approach which can save computing time.

3.3. Hybrid SmEdA/SEA formulation

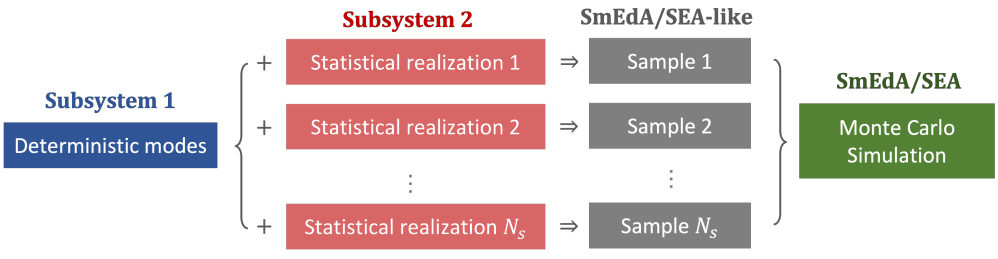

Figure 3: Flow chart of the hybrid SmEdA/SEA approach

The hybrid SmEdA/SEA formulation is developed using a Monte Carlo simulation as shown in the flowchart of Fig. 3. For the structure/cavity system, the deterministic modes of the structure (subsystem 1) can be computed using any available method (for example analytical solutions for academic structures or finite element models for more complex cases) while for the cavity (subsystem 2) the realizations of natural

frequencies and blocked mode shapes on the coupling surface can be obtained through the process detailed in the section 3.2. This process is repeated N_s times to generate a set of different realizations for the purpose of characterizing the randomness as much as possible. For each element of this set, a SmEdA/SEA-Like analysis is performed. This set of SmEdA/SEA-Like analyses forms the samples for the Monte Carlo simulation, upon which, the ensemble average response can be calculated along with the confidence interval generated by the uncertainty and randomness.

As the modes of the equivalent stochastic cavity are constructed based on GOE matrix theory, the number of modes in each statistical realization can slightly vary. Assuming the number of modes in the sth realization is $\bar{N}_2$ ($\bar{N}_2 \approx N_e$), the averaged modal coupling coefficient between mode p of structure and all the $\bar{N}_2$ modes of the cavity approximates to

$$\gamma_p^s \approx \frac{1}{\bar{N}_2} \sum_{\bar{q}=1}^{\bar{N}_2} \beta_{p\bar{q}}. \tag{32}$$

Then, for the s^{th} system sample ($s \in [1, N_s]$) consisting of the deterministic modes of subsystem 1 and the s^{th} statistical realization of subsystem 2, the energy conservation equation of the SmEdA/SEA-like model becomes

$$\begin{aligned} \Pi_{\text{inj}}^p &= \left(\eta_p \omega_p + \bar{N}_2 \gamma_p^s\right) E_p^s - \gamma_p^s E_2^s, \qquad \forall p \in [1, N_1], \\ \Pi_{\text{inj}}^2 &= -\sum_{p=1}^{N_1} \bar{N}_2 \gamma_p^s E_p^s + \left(\sum_{p=1}^{N_1} \gamma_p^s + \eta_2 \omega_c\right) E_2^s, \end{aligned} \tag{33}$$

in which E_p^s and E_2^s denote the modal energy of mode p of the structure and the total energy of the cavity for the s^{th} sample. Then the frequency average total energy of the structure of the s^{th} sample and the frequency average exchanged power between two subsystems can be calculated with

$$E_1^s = \sum_{p=1}^{N_1} E_p^s, \qquad \Pi_{12}^s = \sum_{p=1}^{N_1} \gamma_p^s \left(\bar{N}_2 E_p^s - E_2^s\right). \tag{34}$$

The database of the Monte Carlo simulation can be established with the total energy of subsystem 1 $\left\{E_1^1, ..., E_1^{N_s}\right\}$, the total energy subsystem 2 $\left\{E_2^1, ..., E_2^{N_s}\right\}$ and the exchanged power between two subsystems $\left\{\Pi_{12}^1, ..., \Pi_{12}^{N_s}\right\}$. The ensemble average of each output can be calculated with

$$\overline{X} = \frac{1}{N_s} \sum_{s=1}^{N_s} X^s, \tag{35}$$

where X^s represents one particular element of a dataset in Joule or Watt. The interval in which 95% outputs are expected to fall within (referred as 95% confidence interval in the following) are defined as the zone bounded by its 2.5% and 97.5% percentile. The results are expressed in dB with the reference value $X_{ref} = 10^{-12}$ J for the energies or $X_{ref} = 10^{-12}$ W for the power exchanged.

4. Numerical applications

4.1. Description of the test case

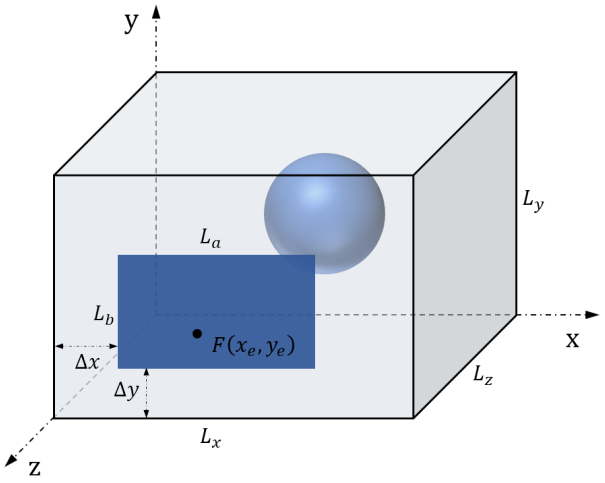

Figure 4: A simply supported plate excited by a point force and coupled to a cavity containing a rigid sphere at an uncertain position.

The vibroacoustic system considered for the numerical applications is presented in Fig. 4. It consists in a simply supported plate of dimensions $L_a = 0.38$ m and $L_b = 0.31$ m and of thickness $h = 1$ mm excited by a random point force F of white-noise type at position $(x_e, y_e) = (0.23, 0.11)$ m. It is coupled to a cavity of dimensions $L_x = 0.48$ m, $L_y = 0.45$ m and $L_z = 0.465$ m. The left bottom corner of the plate is located according to the left bottom corner of the cavity at $\Delta x = 0.068$ m and $\Delta y = 0.11$ m. The plate is made of steel whereas the cavity is filled of air. The Young's modulus, the Poisson ratio and the mass density of the steel are, respectively, $E = 2.1 \times 10^{11}$ Pa, $\upsilon = 0.31$ and $\rho = 7800$ kg/m^3. The mass density and the sound speed of the air are respectively $\rho_{\text{air}} = 1.29$ kg/m^3 and $c_{\text{air}} = 340$ m/s. The damping loss factor for both subsystems is supposed constant with frequency. It is set to $\eta = 0.01$ for the plate and $\eta_{\text{air}} = 0.001$ for the cavity. A rigid sphere of radius $r = 0.15$ m is placed inside the cavity at an uncertain position $(x_s, y_s, z_s) \in [r; L_x - r] \times [r; L_y - r] \times [r; L_y - r]$. This sphere disrupts the neatly arranged modes in the rectangular cavity and it is the source of uncertainty in the present system (like an object can be a source of uncertainty inside a room of a building or a passenger cavity of an automotive). Its position is chosen uniformly distributed in the 3 directions. A population of the uncertain vibroacoustic systems is them considered. Each element of this population corresponds to the a given position of the sphere.

In the proposed hybrid SmEdA/SEA approach, the plate is described as a SmEdA subsystem with its deterministic modes (calculated analytically) whereas the cavity is described as a SEA subsystem with properties corresponding to an equivalent stochastic cavity as described in section 3.2. The results of the

hybrid SmEdA/SEA results should be compared to the energy responses of the population of the considered system. For this purpose, the energy response should be estimated for some element of the population. Finite element simulations have been carried out with the ACTRAN software. For each element of the population, a finite element mesh has been built and the frequency energy responses of the plate and the cavity have been computed. The meshing size is set to be smaller than $1/8$ of the shortest wavelength in each subsystem respectively. For the third-octave band from 565 Hz to 3150 Hz, the meshing size is 3.2mm for the plate and 8mm for the cavity. Consequently, there are about 895000 nodes in the cavity and 11500 nodes in the plate. The frequency step is set to be smaller than $1/6$ of the smallest damping bandwidth, which is 0.5 Hz. As a result, there are 5930 steps for the simulation from 565 Hz to 3150 Hz. Even if using a server with strong computing power [2] and setting parallel computing with 4 cores, it takes more than 1 week to compute one element of the population of the uncertain system. The results of the hybrid SmEdA/SEA approach will be compared in a first step to the results concerning three elements of the population chosen arbitrary: Element 1: $(x_s, y_s, z_s) = (0.22, 0.25, 0.18)$ m, Element 2: $(x_s, y_s, z_s) = (0.28, 0.18, 0.17)$ m, Element 3: $(x_s, y_s, z_s) = (0.26, 0.21, 0.19)$ m.

As previously discussed, the equivalent stochastic cavity considered in the hybrid SmEdA/SEA approach assumes a diffuse field. It can then be expected that the comparison between the hybrid SmEdA/SEA approach and the FEM simulations are in accordance for a frequency above which a diffuse field is achieved in the cavity. The boundary diffuse field index $\overline{\text{BDFI}}$ defined by Chazot et al. [33] is an indicator to evaluate the degree of diffuseness of an acoustic field on a rigid surface. When $\overline{\text{BDFI}}$ is close to 2, the acoustic field on the considered surface (i.e. the coupling surface) can be considered as diffuse. Fig. 5 illustrates the boundary diffuse field index of the three elements of the population defined previously. It can be observed for the 3 elements that the field can be considered as diffuse from the third-octave band centered on 1600 Hz.

[2] 2 processors Intel(R) Xeon(R) 2.20Ghz with 256 Go RAM

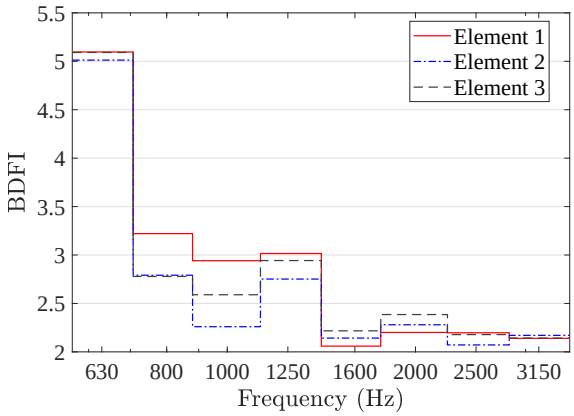

Figure 5: Boundary diffuse field index of three elements of the population of the uncertain vibroacoustic systems.

4.2. Representativeness of the equivalent stochastic cavity

The equivalent stochastic cavity is considered to describe the SEA subsystem in the hybrid SmEdA/SEA approach in order to generate the modal frequencies and modes shapes of this system. In the present section, we are going to study the representativeness of these generated quantities by comparing them to the ones corresponding to the three elements of the population of the system as described in the section 4.1. In each simulation, the meshing size is set to be smaller than 1/8 of the wavelength in the cavity.

4.2.1. Modal frequencies

As shown in Fig. 6(a)-(c), the probability density distributions of the local eigenvalue spacings in the 3150 Hz third-octave band for the three elements of the population follows a Wigner distribution instead of a Poisson distribution. The corresponding equivalent natural frequencies generated by the equivalent stochastic cavity produce the probability density distributions plotted in Fig. 6(d)-(e), here for three different realizations. They clearly produce natural frequencies that follow the same Wigner distribution. It can be noticed that neither the three elements of the population of the real uncertain system nor the three realizations of the equivalent stochastic cavity exhibit a fixed number of modes. The three elements of the population have respectively 208, 207 and 209 modes while the three realizations of the equivalent stochastic cavity generate 209, 206 and 204 modes. Nevertheless, the variability on the number of modes is small and of the same magnitude for both approaches reinforcing the hypothesis that the natural frequencies generated by the equivalent stochastic cavity are representative of the population of the real uncertain system.

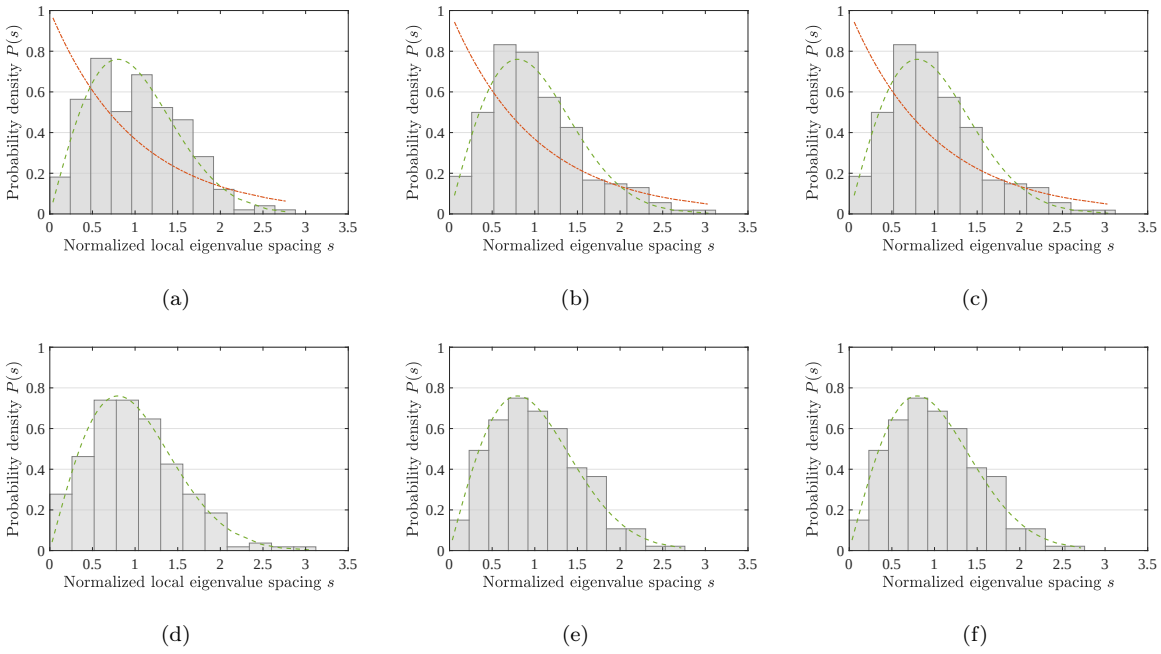

Figure 6: Probability density distributions of local eigenvalue spacing in the third-octave band of central frequency 3150Hz: (a-c), distributions for the elements #1 , #2, #3 respectively; (d-f): distributions of three realizations of the equivalent stochastic cavity; dashed green curve: Wigner distribution; dash-dotted red curves: Poisson distribution.

4.2.2. Representativeness of the equivalent modes shapes

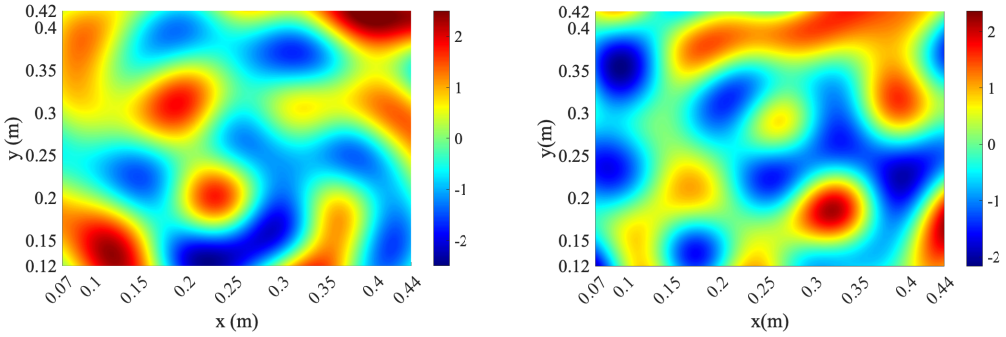

Figure 7: Examples of mode shape realizations of the equivalent stochastic cavity with: (a), the spatial approach; (b), the wavenumber approach. Results on the coupling surface between the plate and the cavity for the third-octave band of central frequency 3150 Hz.

Realizations of mode shapes for the equivalent stochastic cavity can be generated by both the spatial approach and the wavenumber approach. The results are expected to be the same but the CPU time may be different. To validate this, 100 mode shape realizations in the $f_c = 3150$ Hz third-octave band are generated

respectively by these two methods and one example of each method is illustrated in Fig. 7. By comparing Fig. 7(a) and 7(b), it can be seen that the mode shapes generated by spatial and wavenumber approaches share similar wavelength and spatial variation features. In addition, generating 100 realizations by using the spatial approach takes 95 s while it only takes about 1.27 s using the wavenumber approach. Therefore, the results regarding the equivalent stochastic cavity in the following numerical simulations are computed with mode shapes generated by the wavenumber approach.

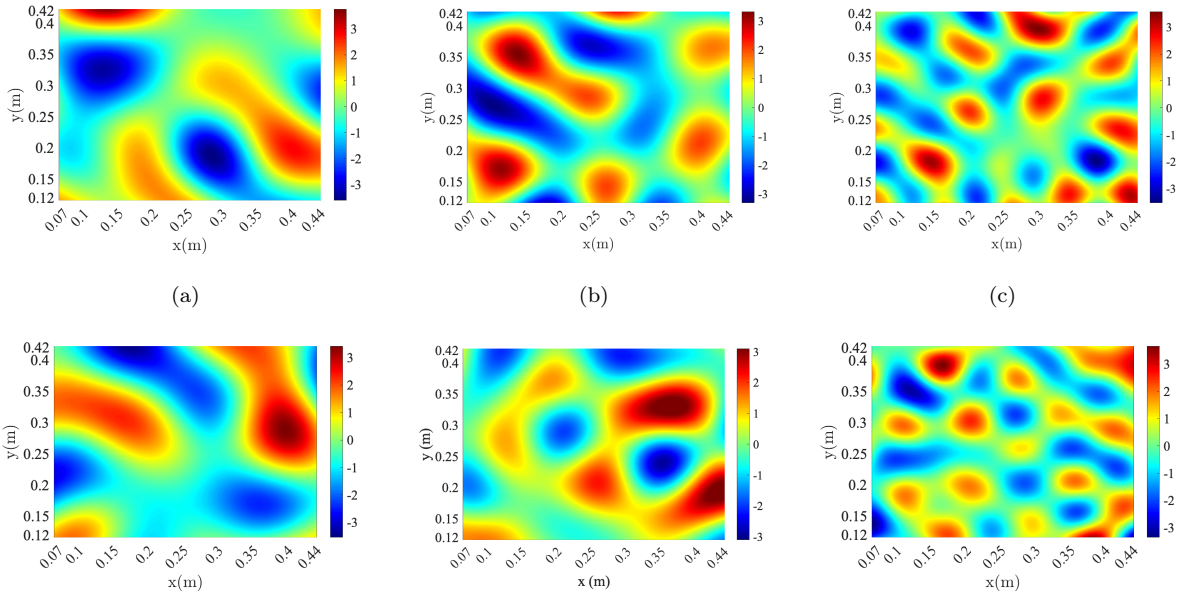

Figure 8: Examples of mode shapes for: (a-c), the elements #1 , #2, #3 of the uncertain cavity respectively; (d-f): three realizations of the equivalent stochastic cavity. Results on the coupling surface for the third-octave band of central frequency: (a,d), 2000 Hz; (b,e), 2500 Hz; (c,f), 4000 Hz.

Fig. 8 shows a mode shape on the coupling surface for each of the three elements of the population of the real uncertain system (Fig. 8 (a)-(c) for elements 1, 2, and 3, respectively) and three mode shape realizations of the equivalent stochastic cavity (Fig. 8 (d)-(f)) in the frequency bands centered on $f_c = 2000$ Hz, 2500 Hz and 4000 Hz respectively. Again, it can be observed that the equivalent stochastic cavity generates mode shapes showing similar wavelengths and amplitudes compared to the one observed in the population of the real uncertain system.

4.2.3. Representativeness of the equivalent interaction modal works and modal coupling loss factors

In the hybrid SmEdA/SEA process, the interaction modal works have to be computed with the analytical plate modes and the generated modes shapes with using Eq. (3). In Fig. 9 they are compared to those obtained for element 1 of the population of the real uncertain system. In both computations, the deter-

ministic modes of the plate remain the same, the only difference comes from the cavity mode shapes. Even though there are more than 200 modes for both element #1 and the realization of the equivalent stochastic cavity, Fig. 9 only shows the interaction modal works of cavity modes q ordered from 1th to 80th as they are sufficient to illustrate their statistical feature.

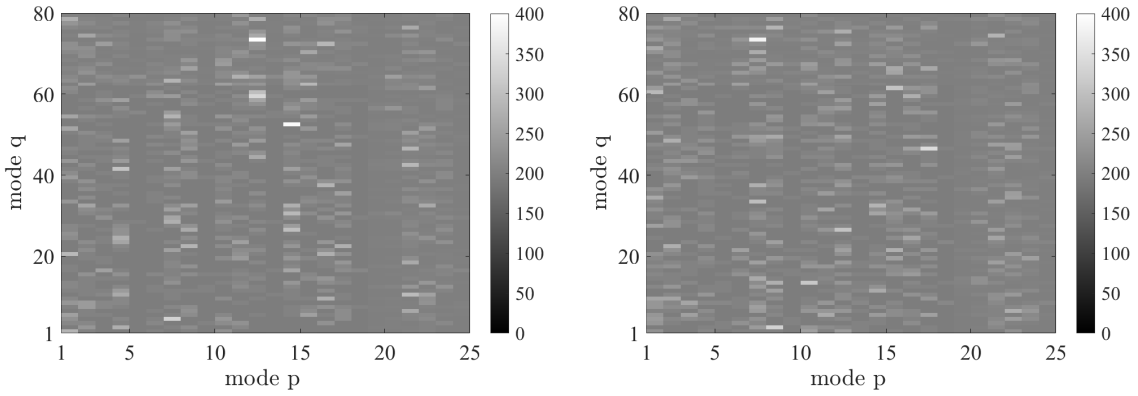

(a) (b)

Figure 9: Interaction modal works between the rectangular plate and: (a), the element #1 of the uncertain cavity; (b) one realization of the equivalent stochastic cavity. Results for the third-octave band of central frequency 3150 Hz.

Obviously, the two results are not expected to be the same. Indeed, a particular mode shape with a particular order generated by the equivalent stochastic cavity can be very different from the corresponding mode shape with the same order computed for element 1 of the population, leading to a different interaction modal work. However, one has to remind that the equivalent stochastic cavity only generates modes statistically equivalent to those of any subsystem with a diffuse field. Each draw of the equivalent stochastic cavity is expected to be different from the real studied case but equivalent on average on several draws. This point will be discussed in the next section. Nevertheless, one can distinguish some common characteristics of the two computations plotted in Fig. 9: some modes of the plate (for mode orders equal to 5, 6, 9, 13, 18, 19, 20, and 24) are less coupled to the cavity compared to the other ones, whatever the description of the cavity modes. This expresses well that some plate modes are weakly coupled to the cavity modes due to non spatial matching.

Introducing these interaction modal works in Eq. (2) permits to compute the modal coupling presented in Fig. 10. Even if the natural frequencies and the modes shapes used in Eq. (2) are generated statistically and share only few features with the real studied system (here the cavity with a sphere inside), the two results are similar. Again, here the comparison is done for only one particular realization of the equivalent stochastic cavity while the process described in Fig. 3 is based on several draws to evaluate the ensemble averages and the 95% confidence intervals. In the next section, the convergence of the approach with respect to the number of draws is investigated.

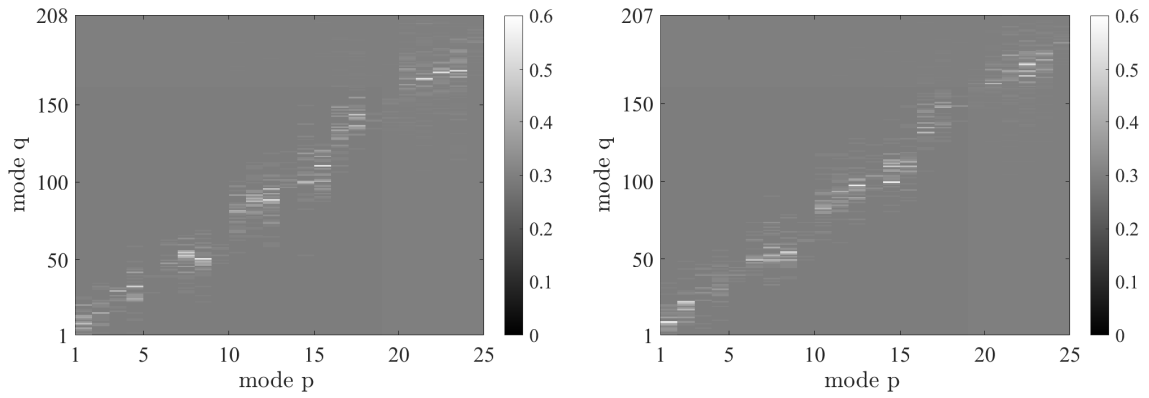

(a) (b)

Figure 10: Modal coupling loss factors between the rectangular plate and: (a), the element #1 of the uncertain cavity; (b) one realization of the equivalent stochastic cavity. Results for the third-octave band of central frequency 3150 Hz.

4.3. Convergence of hybrid SmEdA/SEA formulation

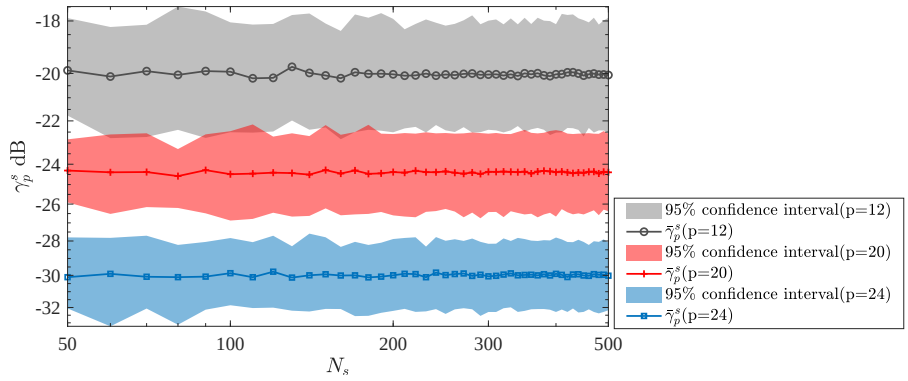

Figure 11: Convergence of the averaged modal coupling coefficient γ_p^s as a function of the number of samples N_s for the plate mode p=12, 20 and 24: expectation, full line; confidence interval: colored area. Results for the third-octave band of central frequency 3150 Hz in dB with $\gamma_{ref} = 1\ s^{-1}$ as reference value.

As described in section 3.2, N_s draws of the equivalent stochastic cavity are considered for estimating the mean and the confidence interval of the energy response of the population of systems. The convergence of the hybrid SmEdA/SEA results as a function of the number of draws, N_s is then studied here. The expectation as well as the confidence interval of the averaged modal coupling coefficient γ_p^s (calculated with Eq. (32)) are plotted in Fig. 11 for three different plate modes (p=12, 20 and 24) as a function of N_s. For the three modes of the plate, the convergence of the averaged modal coupling coefficient is very fast either for the expectation or the confidence intervals. Even if the results stabilize from 200 draws, only a few variations appear for a much smaller number of draws. This point is important because the number of draws directly conditions the computation time.

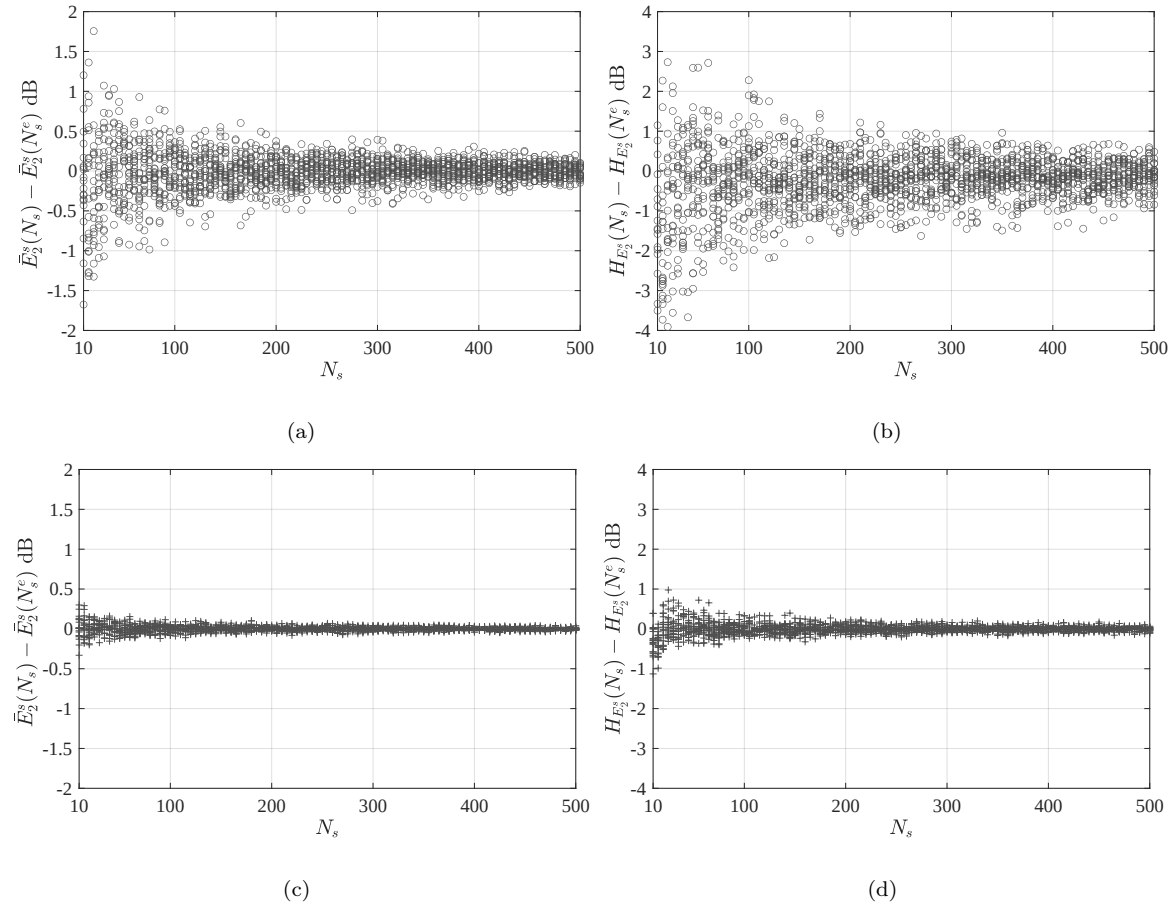

Figure 12: Convergence of energy expectation and confidence interval of the cavity as a function of the number of samples N_s for the third-octave band of central frequency (a,b) 1000 Hz, (c,d) 3150 Hz. (a) the expectation with $\bar{E}_2^s(N_s^e) = 94.2$ dB, (b) the confidence interval with $H_{E_2^s}(N_s^e) = 10.6$ dB. (c) the expectation with $\bar{E}_2^s(N_s^e) = 94.4$ dB, (d) the confidence interval with $H_{E_2^s}(N_s^e) = 1.7$ dB, with the reference value $X_{ref} = 10^{-12}$J.

The final quantities of interest are the subsystem energies because physical quantities like the spatial mean square velocity for the plate or the spatial mean square pressure for the cavity can be deduced from them. As the plate is directly excited by the external mechanical force and that the coupling between the plate and the air cavity is weak, the plate energy can be easily estimated and it is not highly sensitive to the cavity uncertainties. On the contrary, the estimation of the cavity energy is more tricky and is sensitive to the cavity uncertainties. Hence, let us focus on this last quantity. Fig. 12 plots the predicted expectations $\bar{E}_2^s$ and the width of 95% confidence interval $H_{E_2^s}$ (bounded by 2.5% and 97.5% percentile) of the energy as a function of the number of draws. As the values of these two quantities can vary from one set of draws to another, the process is repeated 20 times. This allows studying the dispersion of the results of the proposed model. For each number of draws, the 20 expectations and the 20 confidence intervals are illustrated in the form of subtraction with reference values $\bar{E}_2^s(N_s^e)$ and $H_{E_2^s}(N_s^e)$, which are the results obtained with

$N_s^e = 1000$ samples.

The investigation is proceeded for the third-octave band centered on 1000 Hz in Fig. 12 (a) (b) and on 3150 Hz in Fig. 12 (c) (d). As expected, the variability of the predicted expectations ($\pm \mathrm{Var}_\mu$) and the variability of confidence intervals ($\pm \mathrm{Var}_{\Delta \mathrm{H}}$) decreases with the number of draws. In addition, the convergence of expectation is much faster at 3150Hz than at 1000Hz. The variability at 3150Hz is very small. All the 20 values are between +/- 0.3 dB compared to the reference value with only 10 draws while they are between +/- 0.1 dB with 200 draws. For the width of confidence intervals, the variability is more pronounced but is still acceptable. Indeed, the variability at 1000Hz is larger than at 3150Hz but the reference value of the confidence interval is larger at 1000 Hz than at 3150 Hz. For 200 draws, all the 20 values of the confidence interval compared to the reference value are between +/-1.6 dB at 1000 Hz and +/- 0.3 dB at 3150 Hz whereas the reference value is 10.6 dB at 1000 Hz and 1.7 dB at 3150 Hz. To study more in detail this

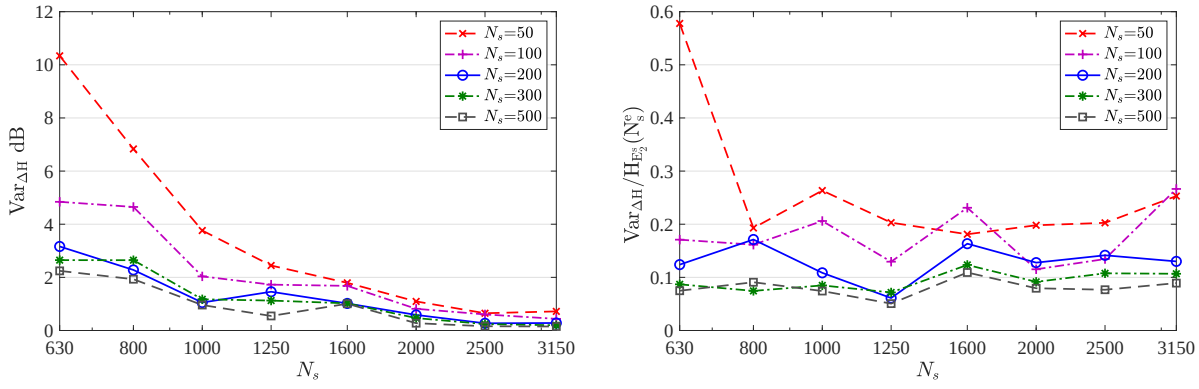

(a) (b)

Figure 13: Convergence of the confidence interval for the cavity energy as a function of frequency: (a), Variability $\mathrm{Var}_{\Delta \mathrm{H}}$ for different number of draws; (b), Ratio between the variability and the reference value $\mathrm{Var}_{\Delta \mathrm{H}}/\mathrm{H}_{\mathrm{E}_2^s}(\mathrm{N}_\mathrm{s}^\mathrm{e})$ for different number of draws.

aspect, the variability $\mathrm{Var}_{\Delta \mathrm{H}}$ of the confidence interval for the cavity energy and the relative variability (the ratio of its variability over the reference value) have been plotted in Fig. 13 as a function of frequency. It can be observed in Fig. 13 (a) that the variability of each frequency band can be reduced by employing more draws (from 50 to 500). Meanwhile, the variability for each number of draws also decreases when the frequency increases. In the lower part of the investigated frequency range, it can take significant values. However, the relative variability does not vary significantly with the frequency. When taking more than 200 draws, the relative variability remains lower than 20% for all the frequency ranges which is satisfactory for the practical applications. 200 draws seems then a good compromise between the accuracy of the calculation and the computing time.

4.4. Hybrid SmEdA/SEA

Focus now on the final results of the hybrid SmEdA/SEA model and their comparisons with the ones obtained by finite element simulations for some elements of the population of uncertain systems. The results plotted in Fig. 14 have been obtained considering 200 draws of the equivalent stochastic cavity. In this figure, it has shown the expectation and the confidence interval (95%) predicted by the hybrid SmEdA/SEA approach as a function of frequency and for the two subsystems. Two main remarks can be made on these results.

- First, the confidence interval of the plate is much narrower than the confidence interval of the cavity. This can be explained by the fact that the plate is directly excited by the external force and that the coupling between the plate and the cavity (filled with air) is weak. It results that the uncertainty of the cavity does not affect significantly the response of the panel which is dominated by the external force and the deterministic mode shapes.

- Second, the confidence interval of the cavity is wider in low frequency and becomes narrower as frequency goes up. As the number of cavity modes and the modal overlap factor increase with frequency, this behavior is expected. In the low frequency bands, the number of modes to be generated for the equivalent stochastic cavity is really low: for instance, there are less than 10 modes in each of the first three frequency bands. Obviously, with such a small number of modes, the variations from one draws to another can be important leading to a large confidence interval. Conversely, in the mid to high frequency bands, more than 60 modes have been generated for each frequency band above 2000 Hz. In this case, the large number of modes leads to natural frequencies covering statistically the entire frequency bands, resulting in less variation in energy predictions and thus a smaller confidence interval (less than +/- 2dB in frequency bands above 2000 Hz). This is in agreement with the $\overline{\text{BDFI}}$ in Fig. 5 which indicates that the diffuse field condition is fulfilled for each element of the population above 1600 Hz.

Fig. 15 shows the comparison between the 95% confidence interval of the exchanged power obtained by the proposed hybrid SmEdA/SEA approach and the frequency average exchanged power computed for 10 elements of the population of the uncertain system (by randomly moving the sphere inside the cavity). The curves for the 10 elements are limited to a maximum frequency of 3530 Hz (third-octave band centered on 3150 Hz) because the computation time became too important beyond this frequency. It is not appropriate to compute the confidence interval with the present FEM results because the number of samples is not sufficient. However, increasing the number of samples would have led to prohibitive computing times. Nevertheless, one can notice that in Fig. 15 the power exchanged predicted by FEM for the 10 elements of

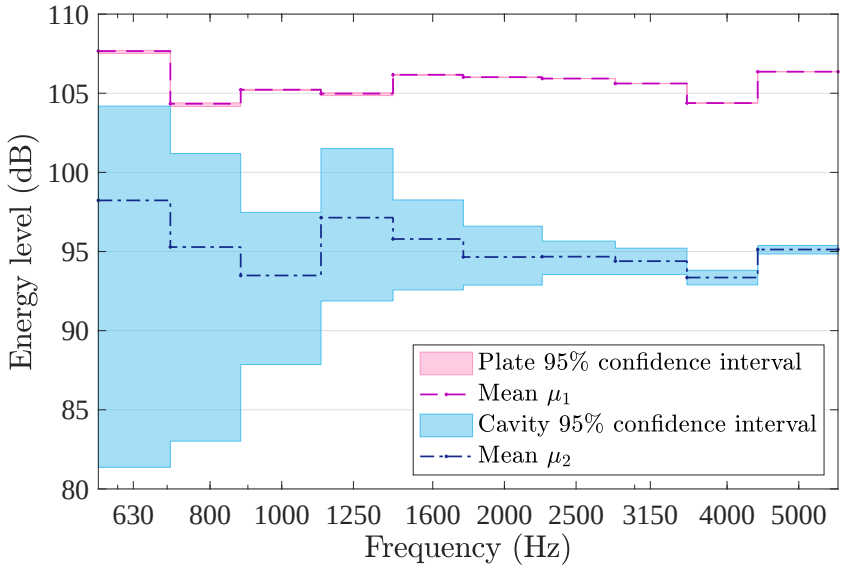

Figure 14: Subsystem energies predicated by the hybrid SmEdA/SEA approach as a function of frequency (dB, ref. 10^{-12} J): Expectation, dash-dotted line; confidence interval, colored area.

the population are well in the 95% confidence interval (excepted for one element in the third-octave 1000 Hz). Moreover, the evolution of the width of the confidence interval as a function of frequency is in agreement with the dispersion of the FEM results which decreases with the frequency. Above 1600 Hz, the confidence intervals are representative of the dispersion of the power exchanged for the 10 elements of the considered population. However, below this frequency, the confidence intervals are not completely consistent with the dispersion of the FEM results. This can be explained by the fact that the uncertainties in the considered population are not large enough to reach, at these frequencies, the state of diffuse field supposed in the hybrid SmEdA/SEA model. Considering a smaller rigid sphere in the cavity would induce smaller variations of the cavity energy in the low frequency whereas a larger sphere would lead to larger variations. As the proposed hybrid SmEdA/SEA approach considers a non-parametric stochastic field, it is not able to describe the effect of uncertainties on particular physical parameters like the sphere radius. However, it is able to give an upper bound of the dispersion of the subsystem energies as long as the acoustic/vibratory field is diffuse in the uncertain subsystem.

As a comparison, the total computation time for direct finite element analysis of the 10 elements of the population of uncertain systems up to the 3150 Hz third-octave band was almost four weeks whereas the total computation of the SmEdA/SEA model (with 200 draws of the equivalent stochastic cavity) up to the 5000 Hz third-octave band was less than 12 hours. Computing the confidence interval with FEM is evidently not possible because its computation time becomes too important as the number of elements increases. By contrast, the computation time for the SmEdA/SEA approach can be further reduced by considering a

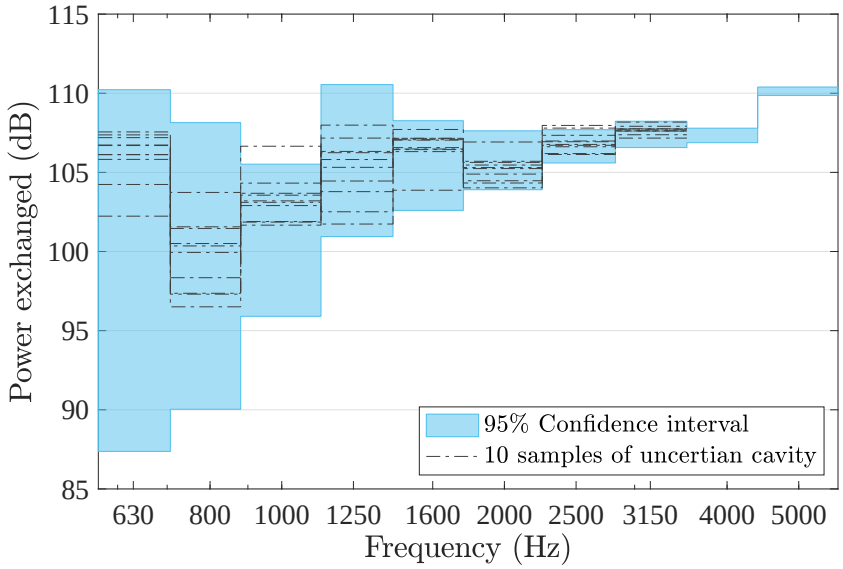

Figure 15: confidence interval of the exchanged power between the plate and the cavity (dB, ref. 10^{-12} W) predicated by the hybrid SmEdA/SEA model (confidence interval in blue) and by FEM for 10 elements of the population (dash-dotted line).

smaller number of draws without a significant modification of the results as seen in Sec. 4.3.

5. Conclusion

The theoretical fundamentals of a hybrid SmEdA/SEA model of a vibroacoustic system have been established in the present paper. Though the presented hybrid model is deduced for a system containing only one deterministic and one statistical subsystem, it can be easily extended to vibroacoustic systems containing more than two subsystems. In this hybrid model, the low modal density subsystem (typically a vibrating structure) is represented deterministically by a SmEdA model and its modes whereas the high modal density subsystem (typically an acoustic cavity) is represented statistically by a SEA model and global physical quantities. For this latter, in addition to the SEA modal energy equipartition assumption, it is supposed that two statistical properties are fulfilled: (a), the distribution of the modal frequency spacings can be related to the distribution of the eigenvalue spacings of a Gaussian Orthogonal Ensemble matrix; (b), the acoustic or vibratory field of the subsystem can be considered as diffuse. Under these assumptions, draws of the modal frequencies and mode shapes of the uncertain subsystem can be easily generated by dedicated processes. For each of these draws, a SmEdA/SEA-like model is then built and solved. Applying a Monte Carlo process, the mean and confidence interval of the subsystem energies can be finally deduced from the energy distribution of the different SmEdA/SEA-like models. This approach has been applied to a test case composed of a plate coupled to a cavity containing a rigid sphere located at an uncertain position. The results are compared to the ones obtained by finite element simulations for ten different positions of the

rigid sphere inside the cavity. Some conclusions can be drawn from the numerical results and the comparison with FEM:

- The mode shapes generated by the equivalent stochastic cavity are representative of those computed by a finite element method. They share the same mode count, probability density distribution the eigenvalue spacing as well as similar wavelengths and amplitudes. These mode shapes can be generated by a spatial approach or a wavenumber approach but this latter is much less computationally expensive. The resulting interaction modal works and modal coupling loss factor used in the SmEdA/SEA model also share similar features compared to the real uncertain cavity with a sphere inside.

- The averaged modal coupling coefficients γ_p^s as well as the mean and 95% confidence interval of the predicted cavity energy converge very quickly. When the number of draws considered is larger than 200, the mean and the confidence interval of the cavity energy become stable with the relative variability of confidence interval lower than 20% for all the frequency ranges.

- The exchanged power results concerning 10 elements of a population of an uncertain system computed by FEM are contained in the 95% confidence interval predicted by the hybrid SmEdA/SEA model. This confirms the effectiveness of the proposed model.

- The proposed model can be used to predict the energy response of an uncertain vibroacoustic system without the need to establish a detailed parameter model for the uncertainty characteristics. It results that the computation time has been greatly reduced compared to a parametric model that can be built from conventional FEM simulations.

The present approach is fully based on an energy representation of the coupling between a deterministic subsystem to a stochastic subsystem. It can be seen as an alternative approach to the hybrid FE-SEA approach which is based on the diffuse field reciprocity relation [17, 18, 19] and the dynamic stiffness representation. These two approaches have similar objectives but with a different base. In the future, the relations between the two approaches will deserve to be studied.

Acknowledgements

The authors are grateful for the financial support of the Up2HF project from Institut Carnot Ingénierie@Lyon. This work was also supported by the LABEX CeLyA (ANR-10-LABX-0060) of Université de Lyon, within the program « Investissements d'Avenir » (ANR-16-IDEX-0005) operated by the French National Research Agency (ANR).

References

[1] O. Zienkiewicz, R. Taylor, J. Zhu, The Finite Element Method: its Basis and Fundamentals (Seventh Edition), seventh edition Edition, Butterworth-Heinemann, Oxford, 2013. doi:10.1016/B978-1-85617-633-0.00002-2.

[2] N. Atalla, F. Sgard, Finite Element and Boundary Methods in Structural Acoustics and Vibration, 1st Edition, CRC Press, Boca Raton, 2015. doi:10.1201/b18366.

[3] M. Wright, R. Weaver, New Directions in Linear Acoustics and Vibration: Quantum Chaos, Random Matrix Theory and Complexity, Cambridge University Press, New York, 2010. doi:10.1017/CBO9780511781520.

[4] R. Lyon, R. Dejong, Theory and Application of Statistical Energy Analysis, Butterworth, London, 1995.

[5] A. Le Bot, Foundation of statistical energy analysis in vibroacoustics, OUP Oxford, 2015.

[6] H. Li, N. Totaro, L. Maxit, A. Le Bot, Ergodic billiard and statistical energy analysis, Wave Motion 87 (2019) 166–178. doi:10.1016/j.wavemoti.2018.08.011.

[7] R. S. Langley, Response variance prediction in the statistical energy analysis of built-up systems, The Journal of the Acoustical Society of America 115 (2) (2004) 706–718. doi:10.1121/1.1642621.

[8] S. Finnveden, Ensemble averaged vibration energy flows in a three-element structure, Journal of Sound and Vibration 187 (3) (1995) 495–529. doi:10.1006/jsvi.1995.0538.

[9] C. Fredö, A SEA-like approach for the derivation of energy flow coefficients with a finite element model, Journal of Sound and Vibration 199 (4) (1997) 645–666. doi:10.1006/jsvi.1996.0634.

[10] H. Hwang, L. Maxit, K. Ege, Y. Gerges, J.-L. Guyader, SmEdA vibro-acoustic modelling in the mid-frequency range including the effect of dissipative treatments, Journal of Sound and Vibration 393 (2017) 187–215. doi:10.1016/j.jsv.2017.01.024.

[11] J. Deng, O. Guasch, L. Maxit, L. Zheng, Transmission loss of plates with multiple embedded acoustic black holes using statistical modal energy distribution analysis, Mechanical Systems and Signal Processing 150 (2021) 107262. doi:10.1016/j.ymssp.2020.107262.

[12] Y. Yu, G. Zhao, S. Ren, Design optimization of mid-frequency vibro-acoustic systems using a statistical modal energy distribution analysis model, Structural and Multidisciplinary Optimization 59 (2019) 1455–1470. doi:10.1007/s00158-018-2139-4.

[13] Àngels Aragonès, L. Maxit, O. Guasch, A graph theory approach to identify resonant and non-resonant transmission paths in statistical modal energy distribution analysis, Journal of Sound and Vibration 350 (2015) 91–110. doi:10.1016/j.jsv.2015.04.001.

[14] K. L. Van Buren, M. Ouisse, S. Cogan, E. Sadoulet-Reboul, L. Maxit, Effect of model-form definition on uncertainty quantification in coupled models of mid-frequency range simulations, Mechanical Systems and Signal Processing 93 (2017) 351–367. doi:10.1016/j.ymssp.2017.02.020.

[15] L. Maxit, J.-L. Guyader, Estimation of SEA coupling loss factors using a dual formulation and FEM modal information, part i: Theory, Journal of Sound and Vibration 239 (5) (2001) 907–930. doi:10.1006/jsvi.2000.3192.

[16] L. Maxit, J.-L. Guyader, Estimation of SEA coupling loss factors using a dual formulation and FEM modal information, part ii: Numerical applications, Journal of Sound and Vibration 239 (5) (2001) 931–948. doi:10.1006/jsvi.2000.3193.

[17] P. J. Shorter, R. S. Langley, Vibro-acoustic analysis of complex systems, Journal of Sound and Vibration 288 (2005) 669–699. doi:10.1016/j.jsv.2005.07.010.

[18] R. S. Langley, J. A. Cordioli, Hybrid deterministic-statistical analysis of vibro-acoustic systems with domain couplings on statistical components, Journal of Sound and Vibration 321 (3) (2009) 893–912. doi:10.1016/j.jsv.2008.10.007.

[19] V. Cotoni, P. Shorter, R. S. Langley, Numerical and experimental validation of a hybrid finite element-statistical energy analysis method, The Journal of the Acoustical Society of America 122 (1) (2007) 259–270. doi:10.1121/1.2739420.

[20] R. Gao, Y. Zhang, D. Kennedy, Application of the dynamic condensation approach to the hybrid FE-SEA model of

mid-frequency vibration in complex built-up systems, Computers and Structures 228 (2020) 106156. doi:10.1016/j.compstruc.2019.106156.

[21] E. Reynders, Generalized reverberant acoustic field modeling based on the gaussian orthogonal ensemble, in: Proceedings of ISMA 2014 International Conference on Noise and Vibration Engineering, KU Leuven Departement Werktuigkunde, 2014, pp. 2341–2356.

[22] C. Van hoorickx, E. P. Reynders, Gaussian orthogonal ensemble modeling of built-up systems containing general diffuse components and parametric uncertainty, Journal of Sound and Vibration 501 (2021) 116045. doi:https://doi.org/10.1016/j.jsv.2021.116045.

[23] L. Maxit, Simulation of the pressure field beneath a turbulent boundary layer using realizations of uncorrelated wall plane waves, The Journal of the Acoustical Society of America 140 (2) (2016) 1268–1285. doi:10.1121/1.4960516.

[24] L. Maxit, J.-L. Guyader, Extension of SEA model to subsystems with non-uniform modal energy distribution, Journal of Sound and Vibration 265 (2) (2003) 337–358. doi:10.1016/S0022-460X(02)01459-1.

[25] L. Maxit, O. Guasch, A dual modal formulation for multiple flexural subsystems connected at a junction in energy-based models, Mechanical Systems and Signal Processing 119 (2019) 457–470. doi:https://doi.org/10.1016/j.ymssp.2018.09.038.

[26] L. Maxit, Analysis of the modal energy distribution of an excited vibrating panel coupled with a heavy fluid cavity by a dual modal formulation, Journal of Sound and Vibration 332 (2013) 6703–6724. doi:10.1016/j.jsv.2013.07.020.

[27] N. Totaro, C. Dodard, J. L. Guyader, SEA Coupling Loss Factors of Complex Vibro-Acoustic Systems, Journal of Vibration and Acoustics 131 (4) (2009) 041009–1. doi:10.1115/1.3086929.

[28] A. Cozza, Stochastic modelling of large cavities : random and coherent field applications, Ph.D. thesis, Université Paris Sud - Paris XI (Sep 2012).

[29] C. Marchetto, L. Maxit, O. Robin, A. Berry, Vibroacoustic response of panels under diffuse acoustic field excitation from sensitivity functions and reciprocity principles, The Journal of the Acoustical Society of America 141 (2017) 4508–4521. doi:10.1121/1.4985126.

[30] M. Karimi, L. Maxit, P. Croaker, O. Robin, A. Skvortsov, S. Marburg, N. Atalla, N. Kessissoglou, Analytical and numerical prediction of acoustic radiation from a panel under turbulent boundary layer excitation, Journal of Sound and Vibration 479 (2020) 115372. doi:https://doi.org/10.1016/j.jsv.2020.115372.

[31] R. K. Cook, R. V. Waterhouse, R. D. Berendt, S. Edelman, M. C. Thompson Jr., Measurement of correlation coefficients in reverberant sound fields, The Acoustical Society of America 27 (1955) 1072–1077. doi:10.1121/1.1908122.

[32] H. Nelisse, J. Nicolas, Characterization of a diffuse field in a reverberant room, The Journal of the Acoustical Society of America 101 (1997) 3517–3524. doi:10.1121/1.418313.

[33] J. Chazot, O. Robin, J. Guyader, N. Atalla, Diffuse acoustic field produced in reverberant rooms: A boundary diffuse field index, Acta Acustica united with Acustica 102 (3) (2016) 503–516. doi:10.3813/AAA.918968.